J. A. Viator and S. A. Prahl, "Photoacoustic imaging of gelatin phantoms using matched field processing," *Laser-Tissue Interaction X: Photochemical, Photothermal, and Photomechanical*, S. L. Jacques, G. J. Müller, A. Roggan, and D. H. Sliney Ed., Proc. SPIE 3601, 276–283, (1999).

Photoacoustic imaging of gelatin phantoms using matched field processing

John A. Viator and Scott A. Prahl[a]

Oregon Graduate Institute of Science and Technology, Portland, OR

Oregon Medical Laser Center, Portland, OR

[a]Oregon Health Sciences University, Portland, OR

ABSTRACT

Matched Field Processing (MFP) has been used in the ocean acoustics community to localize acoustic sources by correlating experimental data with a modelled field based on a solution to the acoustic wave equation. Here we attempt to adapt the method of MFP to localize an acoustic source in a tissue phantom made from an acrylamide gel. An acrylamide gel in a cylindrical geometry was formed with a small optically absorbing sphere embedded within it. A Q-switched, frequency-doubled Nd:YAG laser operating at 532 nm coupled to an optical parametric oscillator (OPO) tuned to 726 nm was used to irradiate the absorbing sphere. The pulse duration was 4.75 ns and the absorption coefficient of the absorbing sphere was 15 cm^{-1}. The stress confined laser energy resulted in an acoustic pulse radiating from the absorbing sphere. A piezoelectric transducer was used to detect the pulses at various locations on the gel. By vertically translating the transducer a virtual hydrophone array was constructed. The acoustic field was modelled using normal mode methods. A simulation was performed using the normal mode model as virtual data which was then correlated with the normal mode model itself. Finally, the experimental acoustic array data was correlated to the normal mode model.

Keywords: matched field processing, acoustic, Q-switched, Nd:YAG, normal model, piezoelectric, transducer

1. INTRODUCTION

Matched Field Processing (MFP) has been developed and used by the ocean acoustics community for over twenty years for localizing acoustic sources in ocean waveguides.[1,2] Seismologists have also used the methods for determining environmental variables in the earth's crust and even non-acoustic applications have been found in electromagnetics.[1] In acoustics, MFP is a method where a modelled field, based on the solution to the acoustic wave equation with appropriate boundary conditions, is correlated to experimentally derived data. When the correlation is high, the modelled field is deemed to be correct, and source location and environmental parameters of the model are assumed to be close to the actual values. Figure 1 shows a typical ocean application where a vertical acoustic array collects acoustic signals from a source. Figure 2 shows a block diagram where the acoustic data is correlated to the modelled field via a correlation processor. The result is a so called ambiguity surface, which simply indicates the level of correlation for putative source locations.

In photoacoustics, a laser source delivers optical energy to an absorber in a stress confined manner *i.e.*, with a pulse duration short enough that all of the optical energy is deposited before any energy can propagate away acoustically. There has been considerable study in biomedical optics regarding this technique.[3–6] Most studies have centered on exploiting knowledge of the acoustic wave to determine the optical properties of the acoustic source. Oraevsky *et al.*[3,4] used a lithium niobate transducer to derive optical properties of tissue phantoms that were purely absorbing and turbid. They also studied layered media. Paultauf *et al.*[5] used a novel optical transducer to derive the absorption coefficient of an absorbing dye solution. Viator *et al.*[6] derived an algorithm for determining the absorption coefficient of layered absorbing media by plane wave analysis of the resultant acoustic wave.

In this paper, we use an MFP method to attempt localization of an optically induced acoustic source in an acrylamide gel cylinder. We used a 4.75 ns pulse from a Q-switched laser to induce the acoustic wave in an absorbing sphere embedded in the gel. We used a piezoelectric transducer to detect the acoustic wave at various positions.

Correspondence: prahl@ece.ogi.edu; (503) 216–2197; http://omlc.ogi.edu

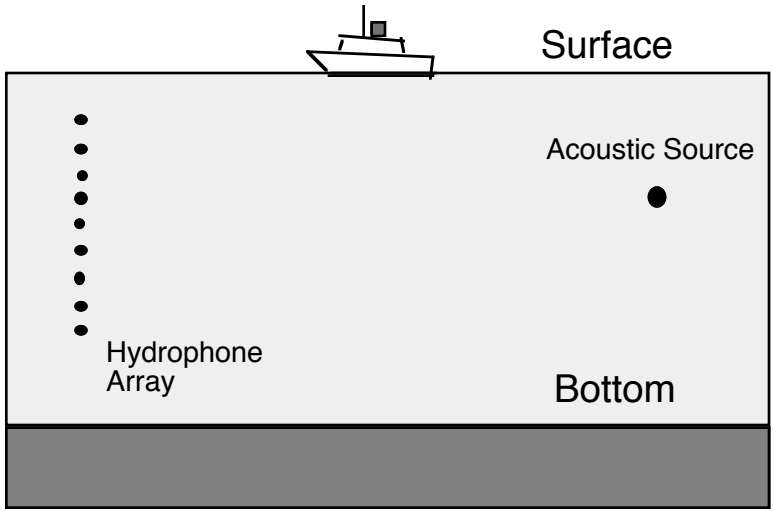

Figure 1. A typical application for MFP. A vertical hydrophone array detects acoustic signals from a distant source. This experimental data is later correlated to modelled data with expected source locations.

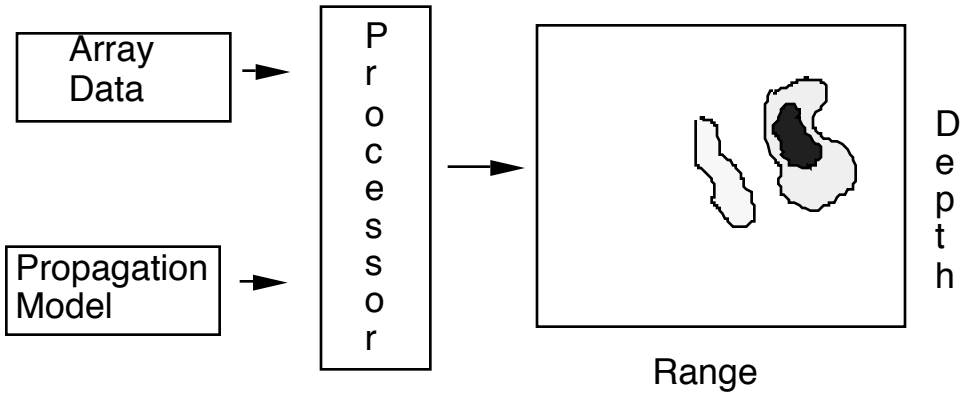

Figure 2. The acoustic array data and the modelled field with predicted acoustic source locations are correlated through a processor. The result is an ambiguity map, where source locations are assigned correlation values. Here the dark areas indicate higher correlations and hence, more probable source locations.

This data set was used as a data vector similar to the data vector from an ocean acoustic array. We used a normal mode model to predict the acoustic field in the acrylamide gel. The model was correlated with the data using a linear processor to derive a correlation curve for the predicted source location. Additionally, we simulated data vectors for various source locations and correlated these vectors with the same modeled field to get correlation curves.

2. Materials and Methods

2.1. Laser

We used a Q-switched, frequency-doubled Nd:YAG laser operating at 532 nm coupled to an optical parametric oscillator (OPO) tuned to 726 nm. The pulse duration was 4.75 ns. The pulse energies varied from 10–13 mJ. The pulse energy was monitored by reflecting a known fraction of the laser beam onto an energy meter prior to entering the fiber face. The laser was launched into a 1000 μm fiber. The output end of the fiber was positioned above the acrylamide gel 5 mm directly above the absorbing sphere. The spot size was circular and 4 mm in diameter.

2.2. Acrylamide Gel

An acrylamide gel was formed by the procedure stated by Sathyam *et al.*.[7] 9.735 g of acrylamide and 0.265 g of bis-acrylamide (Sigma Chemical) were dissolved in 50 ml of deionized water. The addition of a polymerizing initiator of 0.02 g of ammonium persulfate and 0.2 ml of TEMED (Sigma Chemical) created a 20% acrylamide gel. The gel was formed into a cylinder of 23 mm length and 13 mm diameter. An absorbing sphere of 2 mm diameter was embedded in the gel 8 mm along the long axis.

The absorbing sphere in the gel was also formed of acrylamide. The absorber was India Ink (Black ink #723, Eberhard Faber) with an absorption coefficient of 2650 cm^{-1} at 726 nm. The absorption spectrum was without peaks and varied by only 10% over a 50 nm range about 726 nm. The ink was diluted so that the sphere had an absorption coefficient of 15 cm^{-1} at 726 nm. This low absorption coefficient was necessary so that light would be absorbed uniformly in the sphere, so that an acoustic point source was approximated.

2.3. Piezoelectric Transducer

The acoustic transducer was a piezoelectric device with a lithium niobate sensing element (WAT-12, Science Brothers). The transducer had a measured sensitivity of 20 mV/bar. The transducer was fixed to a micropositioner and placed at the circumference of the gel cylinder. The micropositioner translated the transducer in 2.5 mm increments along the long axis of the cylinder. The transducer had a sensing element of 6 mm diameter. To increase the resolution of detection, the sensing area was reduced. A small cylindrical plug of acrylamide gel of about 2 mm diameter was place between the gel phantom and the face of the transducer. This succeeded in increasing the spatial resolution, but decreased transducer sensitivity.

2.4. Experimental Set Up

The set up for the experiments is shown in figure 3. The Q-switched laser beam was split into a known fraction that was used to monitor the pulse energy and the remaining beam that was launched into a 1000 μm fiber. The fiber was positioned 5 mm above the acrylamide gel. The laser beam irradiated the absorbing sphere embedded 8 mm in the cylinder along the long axis. The piezoelectric transducer was translated in 2.5 mm increments along the long axis of the cylinder at circumferential points while the laser was pulsed. The acoustic waveform was detected and recorded on an oscilloscope (DSA 601A, Tektronix). The data was stored and transferred to a computer (Macintosh G3, Apple Computer) for analysis.

2.5. Normal Mode Model of Acoustic Field

A computational solution of the acoustic wave equation can be approached from several avenues, including ray methods, wave number integration, parabolic equation methods, and normal mode methods.[8] The most prevalent method used in the ocean acoustics community, where MFP originated, is the normal mode method. The normal mode method, while not as simple or intuitive as the ray method, is a powerful way to solve the acoustic wave equation and the modes are akin to the frequencies of a vibrating string. The modes determine the wavenumbers which determine frequencies of vibration that are summed to determine the pressure field.

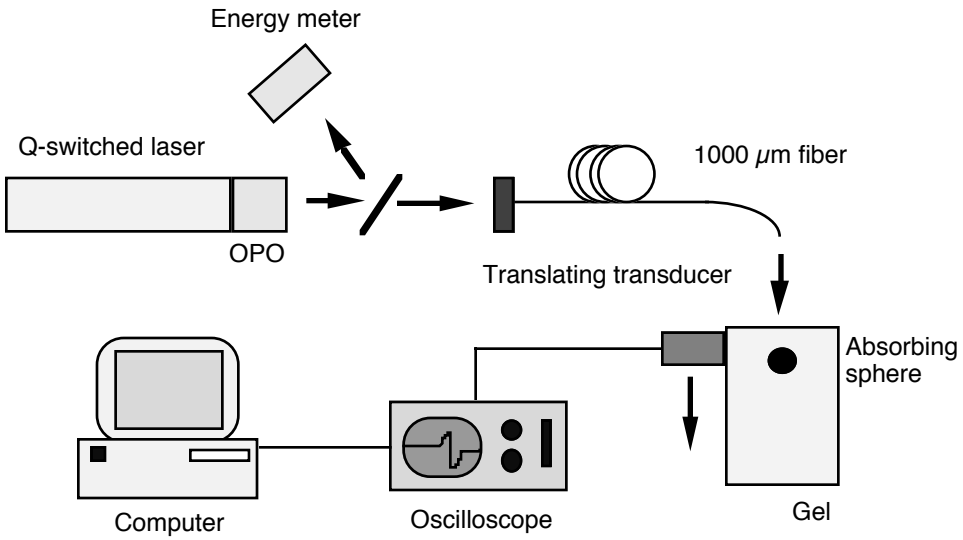

Figure 3. The set up for the MFP experiments. The piezoelectric transducer was translated along the gel surface to create an effective hydrophone array.

In this paper, the acoustic medium of acrylamide gel and can be modeled as an isovelocity problem in ocean acoustics, since the sound speed doesn't change in the acrylamide. The pressure field can be described by[8]

$$p(r,z) = \frac{i}{2D}\sum_{m=1}^{\infty} \sin(k_{zm}z_s) sin(k_{zm}z) H_0^{(1)}(k_{rm}r) \tag{1}$$

where $p(r,z)$ is the pressure field in range r, and depth z, from the receiver D is the depth of the waveguide, k_{zm} is the vertical wavenumber, and $H_0^{(1)}(k_{rm}r)$ is the Hankel function. For computation, we considered only those modes that were deemed propagating, *i.e.,* those with real valued wavenumbers. If the wavenumber is imaginary, then the Hankel function becomes a decaying exponential that drops off rapidly with range. Such a mode is called *evanescent.* The wavenumber is described by the equation

$$k_{rm} = \sqrt{\frac{\omega^2}{c^2} - [(m-\frac{1}{2})\frac{\pi}{D}]^2} \tag{2}$$

where ω is the frequency of the acoustic wave, c is the sound speed in acrylamide, and m is the mode number (any positive integer). The frequency was chosen based on the absorption depth of the laser pulse. In these experiments ω was 5 MHz. When the first term in the radical is less than the second, the wavenumber becomes imaginary and the modes become evanescent.

The pressure field was implemented in MATLAB code for computation of the predicted field used in MFP.

2.6. Linear Matched Field Processor

Many processors exist in the area of MFP, including several nonlinear processors that are designed to increase localization resolution and suppress false correlations. The original processor is the linear, or Bartlett, processor. It is stated as

$$P_{lin} = wC\hat{w}^{\dagger} \tag{3}$$

where P_{lin} is the processor power, w is the normalized experimental data vector, C is the cross spectral density matrix, $\hat{w}$ is the normalized computed field vector, and † indicates the conjugate transpose. The processor power doesn't refer to an actual power, but is the prevalent terminology indicting the degree of correlation, having values from 0 to 1.

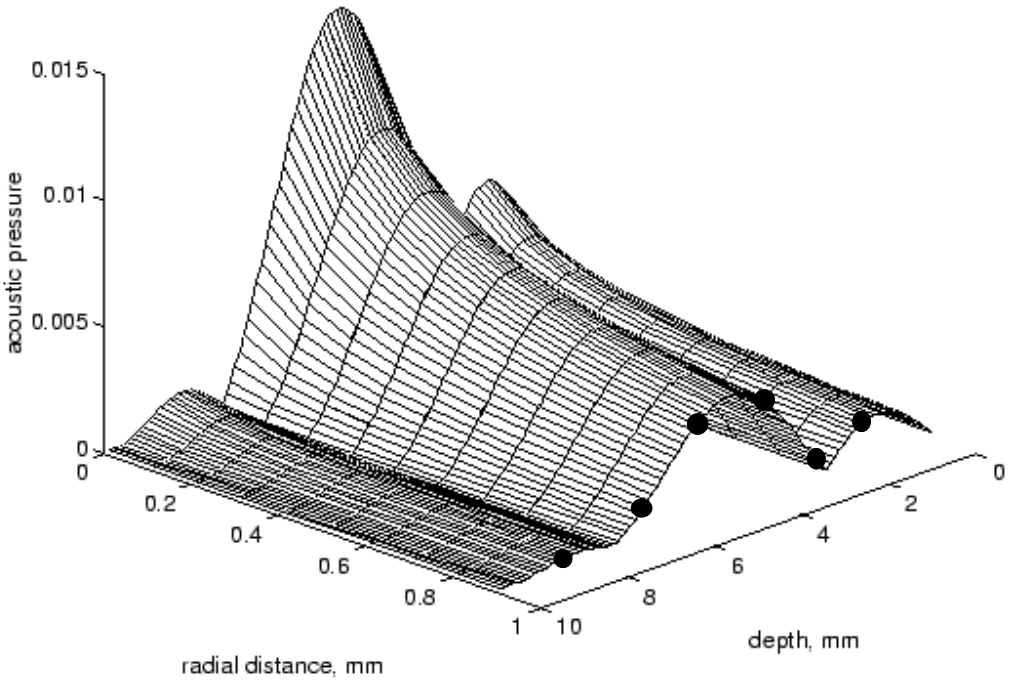

Figure 4. A graphical representation of the modeled acoustic field with an acoustic source at 5.0 mm depth. The black circles indicate sample locations that make up components of the modeled field vector.

In this paper, the linear processor is used in its simplest form, that of a dot product between two normalized vectors. Recalling from vector calculus that the dot product of two vectors is equivalent to determining the projection of one vector onto another, it is clear that a vector would project itself entirely onto another co-linear vector. Hence for normalized vectors, two co-linear vectors would have a dot product of 1. Two orthonormal vectors would have a dot product of zero, indicating no correlation in MFP terminology. In this paper we treated the cross spectral density matrix as a term of unity.

2.7. Computer Simulations

We conducted three simulations localizing acoustic sources in a cylindrical gel of 10 mm length and 10 mm radius. The acoustic field was derived from the normal mode analysis of the acoustic wave equation noted above. The acoustic sources were place on the long axis at depths 2.5, 5.0, and 7.5 mm for the three simulations. A graphical representation of the acoustic field for a 5.0 mm deep source is shown in figure 4. These three acoustic fields were sampled at 10 points in a virtual hydrophone array placed at 10 mm radius and from 0.5 mm depth to 0.95 mm depth in increments of 0.1 mm. These fields were then correlated to the predicted acoustic fields of varying source locations. The correlation was calculated for the source varying in depth only, since the range of the source was well characterized by the location of the laser irradiation, thus saving tremendously on computation.

2.8. Experimental Data

The absorbing sphere in the acrylamide gel was irradiated with the laser, creating an acoustic wave which was detected by the transducer. The laser was pulsed a total of six times with the acoustic transducer translated 2.5 mm in depth with each pulse. This created a virtual hydrophone array. This array data constituted the experimental data vector. At each sampling point, a single acoustic wave was recorded originating from the pulse. Only the peak amplitude was recorded and correlated with the peak amplitude of the modeled field as shown in figure 4.

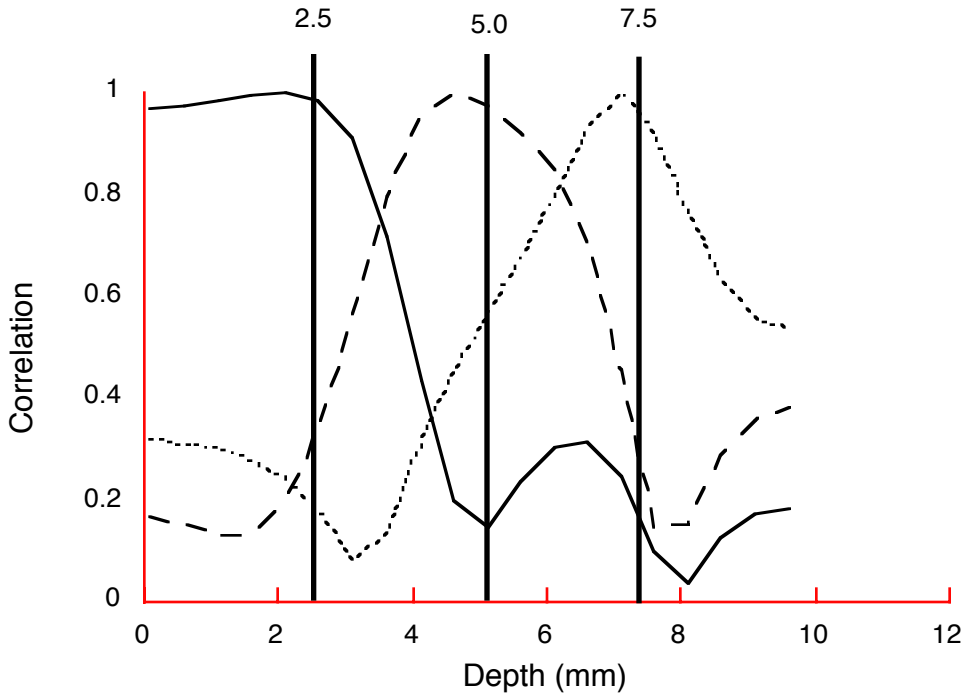

Figure 5. The correlation curve for the predicted depth of the 2.5, 5.0, and 7.5 mm deep acoustic sources. There are side lobes of correlation apart from the main lobes of the actual source locations, due to sampling inaccuracies.

3. Results

3.1. Computer Simulations

The results of the computer simulations are shown in figure 5. The correlation curves are slices of the correlation surface at a range of 5 mm. The correlation peaks of the 2.5, 5.0, and 7.5 mm sources are indicated by the labeled vertical lines.

3.2. Experimental Data

The result of the MFP experiment is shown in figure 6. The correlation curve is a slice of the correlation surface at range 6.5 mm.

4. Discussion

4.1. Computer Simulations

The simulations found high correlation at or near the source locations. The peaks had values of 1.0, indicating perfect correlation between the experimental data and modeled field at that point. However, for the 2.5 mm source depth, there were surface boundary effects that indicated a high false correlation from the depths 0–2.5 mm. While the surface boundary, being a reflective boundary, caused a high pressure field near the surface, the source was absent from these depths. The 2.5 mm deep source also indicated lower correlation sidelobes at 6.0 mm and at the bottom of the waveguide. The 5.0 mm source also showed lower correlation sidelobes. The 7.5 mm source had a lower correlation sidelobe from the surface to about 2 mm and a bottom boundary effect, similar to the 2.5 mm source.

The simulations could possibly have been improved at the cost of computational burden by two ways. First, by increasing the acoustic field sampling by increasing the number of hydrophones and second, by increasing the source location guesses, by increasing the number of modeled acoustic fields. While increasing the number of hydrophones is of small consequence computationally, its benefit may be to reduce the sidelobes evident in the correlation curves. Increasing the number of source location guesses requires the computer to calculate entirely new acoustic fields for

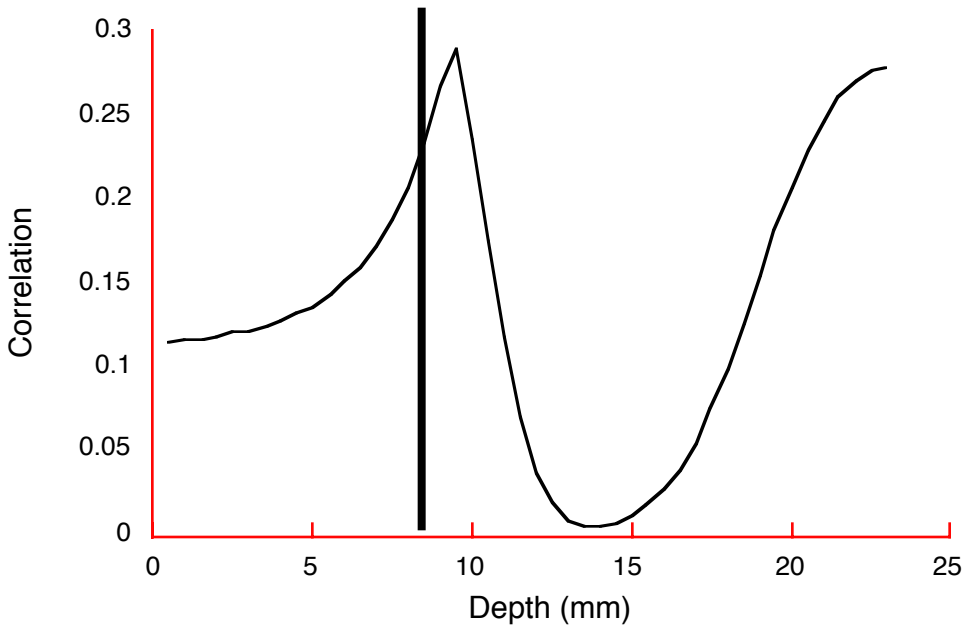

Figure 6. The correlation curve for the predicted depth of the acoustic source in the MFP experiment. The actual location is about 2 mm off of the true location, which is approximately the diameter of the source itself. There is also a large false correlation near the bottom of the gel cylinder. Peak correlations are only 0.3 of a possible 1.0.

each source location guess. This is by far the greater computational burden, but the result should be higher resolution in the correlation curve.

4.2. Experimental Data

The experimental data's correlation curve suffered from low correlation values at the peaks and a large false correlation at the bottom. The peak correlation values, while being clearly delineated peaks, have values of only 0.3. The peak at 10 mm is resolved well, though the peak misses the true source depth at 8 mm depth. The bottom of the acrylamide gel has a broad false peak with value 0.3. There is also a surface boundary effect, similar to that seen in the simulations with a low correlation between the peak at 10 mm and the surface. Problems encountered in gathering the experimental data include poor resolution at the transducer face. The face had a diameter of 6 mm, and though the gel plug that coupled the gel cylinder to the transducer had a diameter of about 2 mm, the resolution will always be limited to this sensing area. Additionally, no time information was used in the correlation. The data vector was composed only of the peak amplitudes and correlated with the amplitudes of the modeled field. If time information had been preserved and incorporated into the model, better localization could have been achieved. Finally, the choice of the normal mode model was not optimal, since the ray method would have been much simpler and allowed more acoustic fields to be modeled.

4.3. Normal Mode Model

The normal mode model of the acoustic wave equation is most often likened to the modes of a vibrating string. The normal modes in the propagation models in this paper are dependent on the surface and bottom boundaries of the waveguide, as shown by the sine terms in equation 1. These sine terms are dependent on the vertical wavenumbers and the source and receiver depths. This is similar to the modes of a string being dependent on the two fixed ends of the string. However, it is less obvious that a pulsed source can be modeled by a method that is often related to a continuously driven source. It has been shown[9,10] that a pulse source can be described with the normal mode model, the derivation being based on the impulsive source in Lagrangian mechanics.

The ray model of acoustic propagation may be a better choice, since it is less computationally intensive and more intuitive, being similar to the ray model in optics. It is derived from the wave equation, separating the

equation into an eikonal component and a transport component. The eikonal equation relies on a high frequency approximation, which limits its usefulness in ocean acoustics, since most of their applications are less the 1000 Hz. In these experiments, however, the frequency was in the megahertz regime, making the ray equation an appropriate choice, not only for its relevance, but also for its simplicity. Future work in MFP in biomedical acoustics should rely on the ray model.

ACKNOWLEDGMENTS

We wish to acknowledge Lt. Martin Taillefer, RCN for his suggestion of applying the method of MFP to biomedical optics. We also wish to thank Dr. R. Chapman and Dr. R. Kessel of the University of Victoria for their helpful discussions on MFP.

REFERENCES

1. A. Tolstoy, *Matched Field Processing in Underwater Acoustics*, World Scientific, Singapore, 1993.
2. A. B. Baggeroer, W. A. Kuperman, and P. N. Mikhalevsky, "An overview of matched field methods in ocean acoustics," *IEEE J. Oceanic Engineering* **18**, pp. 401–424, 1993.
3. A. A. Oraevsky, S. L. Jacques, R. O. Esenaliev, and F. K. Tittel, "Laser-based optoacoustic imaging in biological tissues," *Proc. SPIE* **2134A**, pp. 122–128, 1994.
4. A. A. Oraevsky, S. L. Jacques, and F. K. Tittel, "Determination of tissue optical properties by piezoelectric detection of laser–induced stress waves," *Proc. SPIE* **1882**, pp. 86–101, 1993.
5. G. Paltauf, H. Schmidt-Kloiber, and H. Guss, "Light distribution measurements in absorbing materials by optical detection of laser induced stress waves," *Appl. Phys. Lett* **69**, pp. 1526–1528, 1996.
6. J. A. Viator, S. L. Jacques, and S. A. Prahl, "Generating subsurface acoustic waves in indocyanine green stained elastin biomaterial using a q–switched laser," *Proc. SPIE* **3254A**, pp. 104–111, 1998.
7. U. S. Sathyam and S. A. Prahl, "Limitations in measurements of subsurface temperatures using pulsed photothermal radiometry," *J. Biomed. Optics* **2**, pp. 251–261, 1997.
8. F. B. Jensen, W. A. Kuperman, M. B. Porter, and H. Schmidt, *Computational Ocean Acoustics*, AIP Press, New York, 1994.
9. I. Tolstoy and C. S. Clay, *Ocean Acoustics*, Acoustical Society of America, New York, 1987.
10. M. A. Biot and I. Tolstoy, "Formulation of wave propagation in infinite media by normal coordinates with an application to diffraction," *J. Acous. Soc. America* **29**, pp. 381–391, 1957.